Available online at www.sciencedirect.com
SCIENCE DIRECT
Journal of Organometallic Chemistry 691 (2006) 1790–1796
Journal of Organometallic Chemistry
www.elsevier.com/locate/jorganchem

Synthesis, structures and preliminary biological screening of bis(diphenyl)chlorotin complexes and adducts: $Ph_2ClSn–CH_2–R–CH_2–SnClPh_2$, R = *p*-$C_6H_4$, CH_2CH_2

Srawan K. Thodupunoori, Israel A. Alamudun, Francisco Cervantes-Lee, Fabiola D. Gomez, Yazmin P. Carrasco, Keith H. Pannell *

Department of Chemistry, University of Texas at El Paso, El Paso, TX 79968-0513, USA

Received 9 December 2005; accepted 10 December 2005
Available online 9 February 2006

Abstract

The reaction between $ClCH_2–R–CH_2Cl$, R = *p*-C_6H_4, and $[Ph_3Sn]^-Li^+$ yields $Ph_3Sn–CH_2–R–CH_2–SnPh_3$ (**1**) in high yield. The related known compound R = CH_2CH_2 (**1a**) is synthesized by the reaction of the di-Grignard reagent $BrMg(CH_2)_4MgBr$ with two equivalents of Ph_3SnCl. Cleavage of a single Sn–Ph group at each tin centre of both compounds using HCl/Et_2O yields the corresponding bis-chlorostannanes $Ph_2ClSn–CH_2–R–CH_2–SnClPh_2$, R = $(CH_2)_4$ (**2**) and R = C_6H_4 (**3**), respectively. Compounds **1**, **2** and **3** are crystalline solid materials and their single crystal X-ray structures are reported. In the solid state both **2** and **3** form self-assembled ladder structures involving alternating intermolecular Cl–Sn···Cl and Cl···Sn–Cl bonded chains at both ends of the distannanes with 5-coordinate tin atoms. Recrystallization of **3** from CH_2Cl_2 in the presence of DMF yields the bis-DMF adduct (**4**) in which no self-assembled structures were noted. Evaluation of the chlorostannanes **2** and **3** against a suite of bacteria, *Staphylococcus aureus*, *Escherichia coli* and *Photobacterium phosphoreum* is reported and compared to the related mono-chlorostannanes $Ph_2(CH_3)SnCl$ and $Ph_2(PhCH_2)SnCl$.

Keywords: Distannanes; Tin chlorides; X-ray structures; Self-assembly; Biocidal activity

1. Introduction

The societal use of organotin materials (OTs) is becoming progressively a historical footnote due to the problem of environmental contamination and their non-selective biological activity [1]. Furthermore, Whalen et al. [2a,2b] recently reported significant concentrations of butyl tins in the blood of a random selection of US residents. In addition the same group observed that OTs had a significant negative impact on the function of human natural killer cells [2a,2c]. Together, these reports present a sobering assessment on the future of OTs. However, since many OTs offer significant industrial utility and promising anti-cancer characteristics including the bis-organotin complexes [3], interest in OTs is still ongoing and justified. Indeed, as noted by Champ [4], there is still a strong need to further investigate such compounds to discern in more detail the various aspects of their bioactivity, with perhaps a goal of synthesizing new OTs that can be more targeted and less environmentally problematical. We report bis-organotin chlorides that exhibit interesting new self-assembled ladder structures and compare their biological activity against a suite of bacteria with their mono-tin analogs.

2. Experimental

All reactions were performed in atmospheres of dry nitrogen or argon using solvents dried by conventional techniques. Triphenyltin chloride was purchased from Gelest and the organic starting materials were purchased from Aldrich. Analyses were performed by Galbraith

* Corresponding author. Tel.: +1 915 747 5796; fax: +1 915 747 5748.
E-mail address: kpannell@utep.edu (K.H. Pannell).

0022-328X/$ - see front matter © 2006 Published by Elsevier B.V.
doi:10.1016/j.jorganchem.2005.12.040

Laboratories; NMR spectroscopy was performed using a Bruker300 MHz spectrometer and crystal structures were obtained using a Bruker SMART APEX CCD diffractometer. Both 1,4-bis(triphenylstannyl)butane (**1a**), and 1,4-bis-(diphenylchlorostannyl)butane (**2**) were synthesized using published procedures [5,6].

2.1. Synthesis of α,α¹-bis(triphenylstannyl)-p-xylene (*1*)

To finely cut lithium wire, 0.8 g (0.115 mol.) in 50 ml of tetrahydrofuran that had been sonicated for 2 h, was added dropwise a solution of Ph_3SnCl (10 g, 0.026 mol.) in 20 ml of tetrahydrofuran at 0 °C over 30 min. After the addition was complete the reaction was stirred at 0 °C for 1 h and then allowed to reach ambient temperature and stirred for 16 h to form a dark green/black coloured solution of $[Ph_3Sn]^-Li^+$.

To the above solution was added a 25 ml THF solution of 2.25 g (0.013 mol.) of *p*-dichloroxylene over 30 min at −55 °C. The suspension was stirred for 1 h at −55 °C and then allowed to reach ambient temperature and stirred for 16 h to form a brown/black solution. The solvent was removed under vacuum and the residue was dissolved in a solvent mixture of dichloromethane/hexanes (10:2), the solution was filtered and concentrated. A white solid was formed and after recrystallization from dichloromethane/hexanes yielded **1**, 9.35 g, 0.0116 mol., 45%: m.p. 165–168 °C. Anal. Calc. (Found): C, 65.71 (65.67); H, 4.76 (4.70).

^{1}H NMR ($CDCl_3$, ppm, *J*, Hz); 7.52–7.27 (30, m, *Ph*), 6.81 [4, m, –CH_2–*Ph*–], 2.94 [Sn–CH_2, ^2J (Sn–H) 67.4.
^{13}C NMR ($CDCl_3$, ppm); 19. 7 (Sn–CH_2, ^1J $^{119/117}$Sn–^{13}C, 342/325); 138.81 (Sn–*Ph*, ^1J $^{119/117}$Sn–^{13}C, 491/469), 137.65 (Sn–*Ph*, ^2J $^{119/117}$Sn–^{13}C, 55/36), 128.68 (Sn–*Ph*, ^3J $^{119/117}$Sn–^{13}C, 49/18), 129.16 (Sn–*Ph*, ^4J $^{119/117}Sn_{avg}$–^{13}C, 11); 136.20 (Sn–CH_2–*Ph*, ^2J $^{119/117}$Sn–^{13}C, 42/17), 128.13 (Sn–CH_2–*Ph*, ^3J $^{119/117}Sn_{avg}$–^{13}C – 12).
^{119}Sn NMR ($CDCl_3$, ppm); −118.7.
IR (cm^{-1}, CCl_4): 3066 (s), 3051 (m), 3018 (m), 2991 (w), 2916 (vw), 1967 (w), 1950 (w), 1892 (w), 1876 (w), 1816 (w), 1579 (vw), 1504 (m), 1429 (s), 1074 (m), 727 (vs), 696 (vs).

2.2. Synthesis of α,α¹-bis(diphenylchlorostannyl)-p-xylene (*3*)

To a suspension of 5.0 g (0.0062 mol.) of **1** in 35 ml of dry dichloromethane was added dropwise 2.0 equiv. of hydrogen chloride in diethyl ether (12.5 ml, 0.0123 mol.) at −55 °C over 30 min. The resulting mixture was stirred at this temperature for 1 h and allowed to reach ambient temperature. After 15 h the solvent was removed under vacuum and the residue was washed with cold hexanes. Purification was performed by recrystallization from dichloromethane/hexanes mixture to yield **3**, 3.75 g, 0.0052 mol., 84%; m.p. 141–143 °C. Anal. Calc. (Found): C, 53.31 (52.92); H, 3.91 (3.95).

^{1}H NMR ($CDCl_3$, ppm): 7.45–7.35 (20, m, Sn–*Ph*), 7.02 (4, m, CH_2–*Ph*), 3.11 [Sn–CH_2,^2J (Sn–H) 73.
^{13}C NMR ($CDCl_3$, ppm, *J*, Hz): 25.43 (Sn–CH_2, ^1J $^{119/117}$Sn–^{13}C, 378/361); 138.07 (Sn–*Ph*, ^1J $^{119/117}$Sn–^{13}C, 552/527), 136.05 (Sn–*Ph*, ^2J $^{119/117}Sn_{avg}$–^{13}C, 46), 129.09 (Sn–*Ph*, ^3J $^{119/117}Sn_{avg}$–^{13}C, 59), 130.37 (Sn–*Ph*, ^4J $^{119/117}Sn_{avg}$–^{13}C,13), 134.30 (Sn–CH_2–*Ph*, ^2J $^{119/117}$Sn–^{13}C, 49/23), 128.49 (Sn–CH_2–*Ph*, ^3J $^{119/117}Sn_{avg}$–^{13}C, 34).
^{119}Sn NMR ($CDCl_3$, ppm): −24.67.
IR (cm^{-1}, CCl_4): 3070 (s), 3053 (s), 3021 (m), 2994 (w), 2923 (bd. vw), 1971 (w), 1954 (w), 1896 (w), 1878 (w), 1817 (w), 1506 (s), 1430 (vs), 1074 (s), 727 (vs), 696 (vs).

2.3. Single crystal structural determination

Crystals of **1**–**4** were mounted on glass fibers. The X-ray intensity data were measured on a Bruker SMART APEX CCD area detector system equipped with a graphite monochromator and a Mo Kα fine-focus sealed tube ($\lambda = 0.71073$ Å). Frames were collected with a scan width of 0.30° in ω and an exposure time of 10 s/frame. The frames were integrated with the Bruker SAINT software package using a narrow-frame integration algorithm. Analysis of the data showed negligible decay during data collection. Data were corrected for absorption effects using the multiscan technique (SADABS). The structures were solved and refined using the Bruker SHELXTL (Version 6.1012) Software Package. The corresponding crystal and refinement data for each compound are summarized in Table 1.

The structure of **3** was first solved at room temperature and showed some disorder in one of the phenyl rings. Data were then collected at 100k and the structure was found to be statically disordered, having one of the phenyl rings in two different orientations. The low temperature data allowed simple modeling of the disorder by splitting the disordered atoms (C6 and C6′, C7 and C7′, C9 and C9′ and C10 and C10′) between the two possible orientations and refining the site occupancy for each atom, keeping the total occupancy for each pair constrained to 1.000 using the SHELXTL software.

2.4. Biocidal evaluation

MIC determinations (NCCLS, M7-A4, 1997) [9].

Stock solutions of the organotin compounds were made 10^{-2} M in DMSO (Aldrich). A tenfold dilution in DMSO of each stock compound was made, providing 10^{-3} M solutions. Twofold serial dilutions of each compound were obtained by using Mueller Hinton broth (Difco Laboratories, Detroit, MI). The resulting concentrations ranged from 10^{-3} to 3.1×10^{-7} M. A 96-well polypropylene microdilution plate was used for each compound. 100 μL of each

Table 1
Crystal and refinement data for compounds **1**–**4**

Compounds	**1**	**2**	**3**	**4**
Identification code	028ST	993IS	S108L	108RT
Empirical formula	$C_{22}H_{19}Sn$	$C_{14}H_{14}ClSn$	$C_{16}H_{14}ClSn$	$C19H_{21}ClNO$
Formula weight	804.12	672.78	684.79	433.51
Temperature (K)	296(2)	296(2)	100(2)	296(2)
Wavelength (Å)	0.71073	0.71073	0.71073	0.71073
Crystal size (mm)	$0.50 \times 0.40 \times 0.40$	$0.32 \times 0.28 \times 0.15$	$0.24 \times 0.20 \times 0.02$	$0.20 \times 0.20 \times 0.14$
Crystal habit	Colorless prism	Colorless plate	Colorless plate	Colorless chunk
Crystal system	Monoclinic	Triclinic	Monoclinic	Monoclinic
Space group	$C2/c$	$P\bar{1}$	$P2(1)/n$	$P2(1)/n$
Unit cell dimensions				
a (Å)	13.175(3)	12.9427(17)	16.0707(12)	9.759(3)
b (Å)	15.080(4)	9.1540(12)	16.4626(12)	13.988(4)
c (Å)	19.667(5)	6.3319(8)	5.6489(4)	13.543(4)
α (°)	90	99.996(2)	90	90
β (°)	108.460(4)	102.505(2)	110.8150(10)	94.018
γ (°)	90	100.884(2)	90	90
V (Å^3)	3706.4(15)	700.99(16)	1396.96(18)	1844.2(9)
Z	8	2	4	4
D_{calc} (Mg/m^3)	1.441	1.594	1.628	1.561
Absorption coefficient (mm^{-1})	1.376	1.985	1.994	1.534
$F(000)$	1608	330	672	868
Detector distance (cm)	5.96	5.97	5.96	5.98
θ Range for data collection (°)	2.12–28.30	1.64–28.27	1.52–28.24	2.10–23.26
Index ranges	$-16 \leqslant h \leqslant 16$, $-20 \leqslant k \leqslant 9$, $-25 \leqslant l \leqslant 23$	$-8 \leqslant h \leqslant 8$, $-12 \leqslant k \leqslant 12$, $-17 \leqslant l \leqslant 16$	$-17 \leqslant h \leqslant 21$, $-6 \leqslant k \leqslant 7$, $-21 \leqslant l \leqslant 17$	$-10 \leqslant h \leqslant 10$, $-15 \leqslant k \leqslant 15$, $-15 \leqslant l \leqslant 15$
Reflections collected	11465	8077	8313	14879
Independent reflections [R_{int}]	4285 [0.0238]	3199 [0.0214]	3248 [0.0274]	2638 [0.0414]
Coverage of independent reflections	92.80%	91.50%	93.90%	99.70%
Absorption correction	SADABS	SADABS	SADABS	SADABS
Maximum/minimum transmission	0.6091/0.5462	0.7550/0.5691	0.9612/0.6461	0.8139/0.7490
Refinement technique	Full-matrix least-squares on F^2	Full-matrix least-squares on F^2	Full-matrix least-squares on F^2	Full-matrix least-squares on F^2
Function minimized	$\sum(F_o^2 - F_c^2)^2$	$\sum(F_o^2 - F_c^2)^2$	$\sum(F_o^2 - F_c^2)^2$	$\sum(F_o^2 - F_c^2)^2$
Data/restraint/parameters	4285/0/208	3199/0/145	3248/0/200	2638/0/210
Goodness-of-fit on F^2	1.21	1.12	1.11	1.192
R_1; $I > 2\sigma(I)$	0.047, 3839 data	0.0299, 3063 data	0.0378, 3034 data	0.0316, 2559 data
wR_2; $I > 2\sigma(I)$	0.1048, 3839 data	0.0722, 3063 data	0.0816, 3034 data	0.0696, 2559 data
R_1 all data	0.0541	0.0316	0.0415	0.0331
wR_2 all data	0.1083	0.0732	0.0834	0.0704
Largest difference in peak and hole (e Å^{-3})	0.481 and −0.896	0.601 and −0.412	1.137 and −0.912	0.493 and −0.386

twofold dilution concentration were placed in triplicate in each well. *Escherichia coli* (ATCC 25922), *Staphylococcus aureus* (ATCC 25923) and *Photobacterium phosphoreum* (ATCC 49387) were obtained from American Type Collection, Manassas, VA and was revived using trypticase soy medium (Beckton Dickinson and Company, Cockeysville, MD). Colonies of *S. aureus* were further transferred weekly to tryptic soy agar plates (Beckton Dickinson and Company, Cockeysville, MD). Three to five, isolated, morphologically similar colonies, were transferred to a tube of 3 mL tryptic soy broth medium (Beckton Dickinson and Company, Cockeysville, MD) and incubated at 37 °C for 1–2 h. A bacterial suspension was made by adding sterile saline solution (0.9%) to the culture. It was further diluted in saline by a factor of 1:10 providing a final population density of $1-2 \times 10^7$ CFU's (colony forming units). The 96-well plate was innoculated with 5 μL of the final bacterial suspension. Incubation of the plate proceeded at 35 °C for 16–20 h. A positive and negative growth controls containing 100 μL of Mueller Hinton broth were present in each plate. The minimum inhibitory concentration (MIC) resulted from recording the lower concentration which inhibited growth.

3. Results and discussion

3.1. Synthesis and spectroscopic characterizations

The formation of the two bis-triphenyltin compounds was successfully accomplished in good yields using standard salt-elimination chemistries denoted in:

$$2[Ph_3Sn]^-Li^+ + ClCH_2\text{–}C_6H_4\text{–}p\text{-}CH_2Cl \rightarrow Ph_3SnCH_2\text{–}C_6H_4\text{–}p\text{-}CH_2SnPh_3\ (\mathbf{1}) \quad (1)$$

$$2Ph_3SnCl + MgBr(CH_2)_4MgBr \rightarrow Ph_3Sn(CH_2)_4SnPh_3\ (\mathbf{1a}) \quad (2)$$

Compound **1** has not been previously reported in the literature whereas **1a** was first synthesized in 1954 via the same route [5]. All spectroscopic data are in accord with the proposed structures. For example, the ^{119}Sn NMR solution spectra exhibit resonances at −118.7 (**1**) and −100.0 ppm (**1a**) in the general range for Ph_3SnCH_2 compounds and the various coupling constants noted in Section 2 are also in total accord with the literature [7].

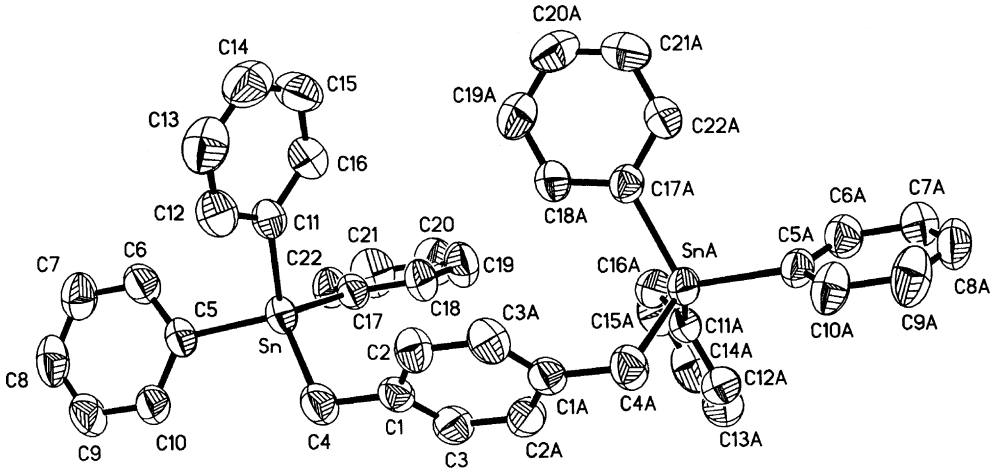

Fig. 1. Molecular structure of $Ph_3SnCH_2C_6H_4$–*p*-CH_2SnPh_3 (**1**).

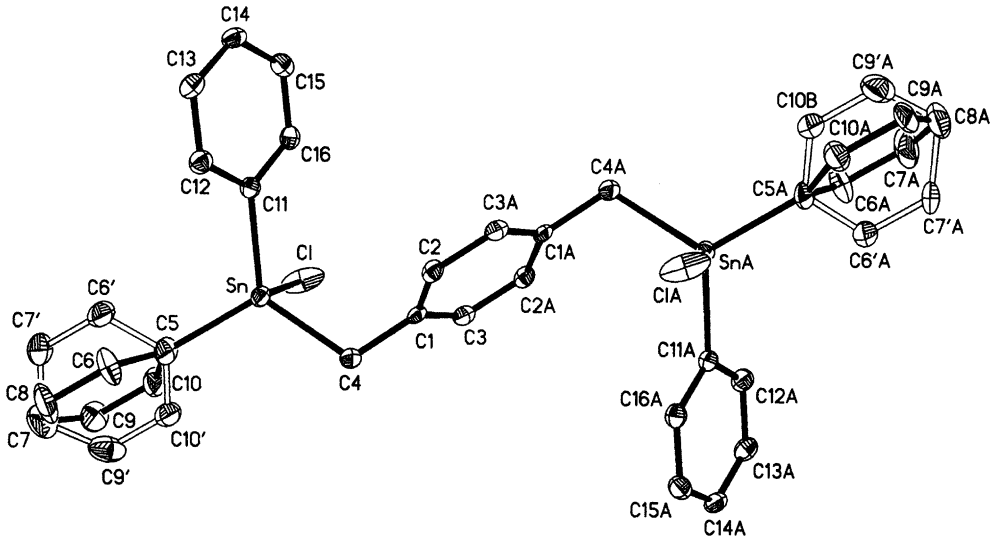

Fig. 2. Molecular structure of $Ph_2ClSnCH_2C_6H_4$–*p*-CH_2SnPh_2Cl (**3**).

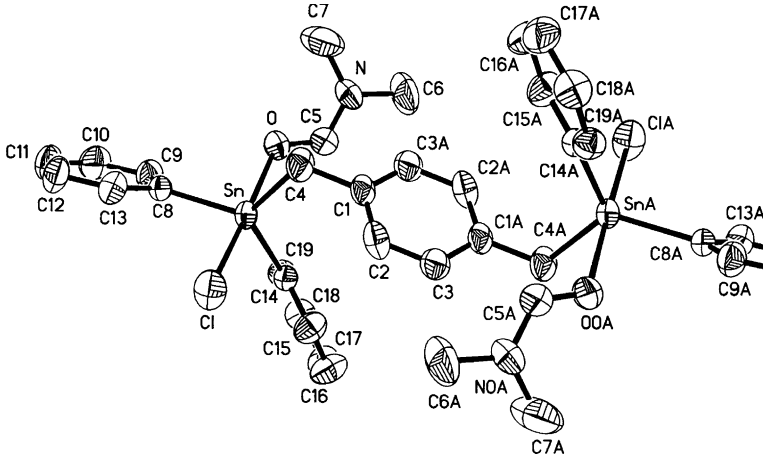

Fig. 3. Molecular structure of $Ph_2ClSnCH_2C_6H_4$–*p*-CH_2SnPh_2Cl $(DMF)_2$ (**4**).

The acid cleavage of aryl–tin bonds is well-established and the commercially available reagent HCl/Et_2O is particularly useful in this regard. The reactions of **1** and **1a** to form **2** and **3** can be monitored by ^{119}Sn NMR and the formation of any bis-chloro compounds held to a minimum. The spectroscopic data of **2** and **3** are in total accord with the proposed structures.

3.2. Single crystal X-ray structural analysis

We have been able to determine the single crystal structures of both the new compounds **1** and **3** and these molecular structures are illustrated in Figs. 1 and 2, respectively, together with a second structural analysis of **3** when coordinated with DMF, Fig. 3. The single crystal structures of both **1a** and **2** have been reported [8,9]; however, in the case of **2** the packing arrangement, now illustrated in Fig. 4 along with that of **3**, was not reported [10].

The simple tetraorganotin compound **1** has a non-remarkable structure as expected. The two stannyl groups are *cis* with respect to the bridging xylyl group, presumably a function of the packing, although no intermolecular interactions are noted in the packing diagram. The selected bond lengths and angles recorded in Table 2 are in the normal ranges for OTs with similar structural units (Table 3).

The related bis-diphenylchlorotin compound **3** shows a distorted tetrahedral structure about the Sn atom due to an intermolecular Cl···Sn interaction, well-known in the

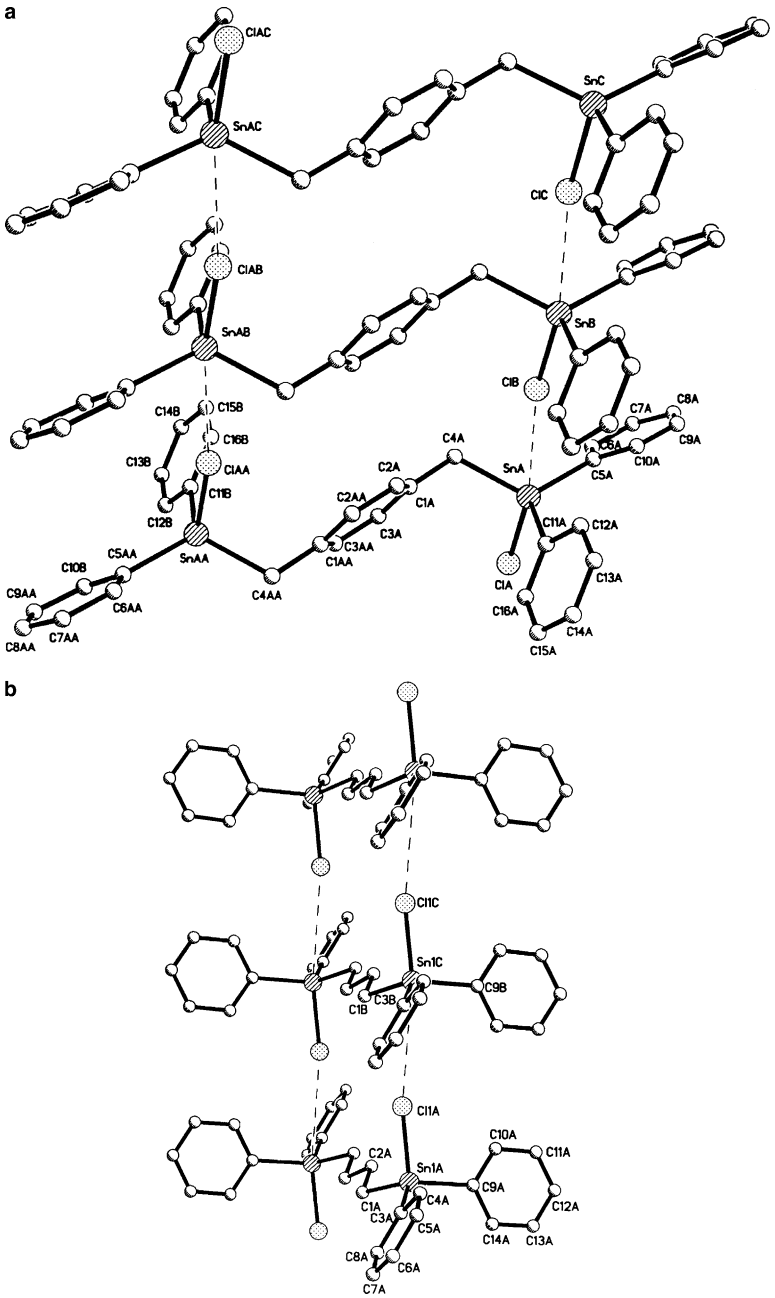

Fig. 4. Packing diagram of **2** (b) and **3** (a) illustrating ladder self-assembled structure.

Table 2
Selected bond lengths (Å)

For **1**			
Sn–C11	2.136(4)	Sn–C5	2.136(4)
Sn–C17	2.143(4)	Sn–C4	2.159(4)
For **2**			
Snl–Cl	2.125(3)	Sn1–C9	2.125(3)
Snl–C3	2.128(3)	Sn1–C11	2.3737(10)
For **3**			
Sn–C5	2.119(4)	Sn–C11	2.122(4)
Sn–C4	2.151(4)	Sn–C1	2.4166(12)
For **4**			
Sn–C14	2.143(4)	Sn–C8	2.143(4)
Sn–C4	2.152(4)	Sn–O	2.412(3)
Sn–Cl	2.4835(13)	O–C5	1.228(5)

Symmetry transformations used to generate equivalent atoms: #1 $-x+1$, $-y$, $-z+2$.

Table 3
Bond angles (°)

For **1**			
C11–Sn–C5	107.11(14)	C11–Sn–C17	107.41(14)
C5–Sn–C17	109.23(14)	C11–Sn–C4	110.06(16)
C5–Sn–C4	111.19(15)	C17–Sn–C4	111.68(16)
For **2**			
C1–Sn1–C9	114.31(12)	C1–Sn1–C3	118.68(11)
C9–Sn1–C3	112.98(11)	C1–Sn1–C11	103.39(9)
C9–Sn1–C11	101.28(9)	C3–Sn1–C11	103.25(9)
For **3**			
C5–Sn–C11	116.15(15)	C5–Sn–C4	116.98(15)
C11–Sn–C4	120.22(14)	C5–Sn–C1	101.85(13)
C11–Sn–C1	99.35(11)	C4–Sn–Cl	94.84(12)
For **4**			
C14–Sn–C8	116.47(14)	C14–Sn–C4	120.13(15)
C8–Sn–C4	121.79(15)	C 14–Sn–O	87.72(12)
C8–Sn–O	84.51(12)	C4–Sn–O	85.17(16)
C14–Sn–C1	94.11(11)	C8–Sn–C1	94.34(11)
C4–Sn–C1	94.21(14)	O–Sn–C1	178.14(7)

Symmetry transformations used to generate equivalent atoms: #1 $-x+1$, $-y$, $-z+2$.

structural analysis of chlorotin compounds [11]. The two stannyl groups are now *trans* with respect to the xylyl group and this arrangement is best noted in the packing diagram, Fig. 4a, where a ladder-like arrangement can be noted. Each tin atom of the molecule is involved in a Cl···Sn interaction with a neighbouring molecule. Furthermore in this interaction one of the two SnCl groups act as donor while the other acts as an acceptor to the specific individual neighbouring molecule. The situation is reproduced throughout the structure to produce the self-assembled ladders. The Sn–Cl covalent bond length is 2.417 Å while the secondary Cl···Sn internuclear distance is 3.252 Å. These distances are similar to those in other Sn–Cl self-assembled bonding situations reported in the literature [11]. For example, in the polymeric structure of Me_3SnCl formed via intermolecular secondary Cl···Sn bonding, the terminal and bridging Sn–Cl distances are reported as 2.430 and 3.269 Å, respectively [12]. Indeed the intermolecular distance in **3** of 3.252 Å is one of the shortest secondary Cl···Sn distances in the literature.

The molecular structure **2** is reported in the literature and it was noted that a degree of Cl···Sn intermolecular bonding occurs; however, no detail was provided. The packing diagram for **2** is shown in Fig. 4b and is remarkably similar to that of **3**. A very clear ladder-like structure is noted involving both SnCl groups acting, as in **3**, as both Lewis acid and Lewis base. Despite this similarity, from the terminal and bridging Sn–Cl distances of 2.373 and 3.989 Å, respectively, indicate that the intermolecular interaction is weaker, i.e., the terminal Sn–Cl bond is shorter, and the intermolecular Cl···Sn internuclear distance greater, than in **3**. The secondary Cl···Sn bonding distance of 3.989 Å is one of the longest reported where self-assembly can be designated and is essentially the sum of the van der Waals radii for Sn and Cl. Although rather longer than usually associated with an intermolecularly assembled situation this value may be compared to those noted in the polymeric structure of $SnCy_2Cl_2$ where the terminal and bridging distances are 2.407 Å (2.371 Å) and 3.332 Å (3.976 Å), respectively [13].

With respect to the nature of the intermolecular self-assembly, a useful measure of such interactions is the angular distortion that results at the tin atom [14]. For example, assuming the Cl–Sn···Cl arrangement to be the incipient axial portion of a trigonal bipyramidal structure, the difference between the sum of the equatorial angles and axial angles would be zero for a tetrahedron and 90° for a trigonal bipyramid. Such an analysis for **3** reveals a $\sum$eq $-$ $\sum$ax of 57.3° and a much smaller value of 38.0° is found for **2**. By way of comparison in this study the corresponding values for the essentially unperturbed **1** is 7°, while the bis-DMF adduct described below is 76°. These data, in conjunction with the various C–Sn and Cl···Sn internuclear distances reveal that a significant self-assembling can be noted when considering the bond angles at tin, even when the Cl···Sn internuclear distances are at, or above, the sum of the van der Waals radii.

The bis-DMF adduct **4** was obtained when **3** was recrystallized from a CH_2Cl_2 solution containing a small amount

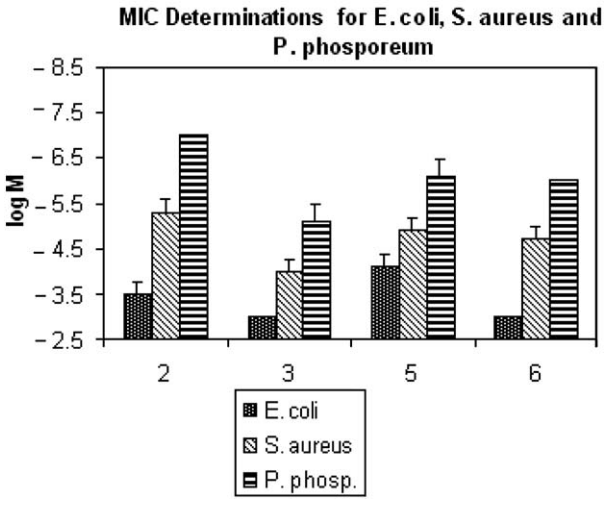

Fig. 5. Minimum inhibitory concentrations of $Ph_2ClSnCH_2$–R–$CH_2SnClPh_2$(**2**,**3**)$Ph_2(CH_3)SnCl$ (**5**) and $Ph_2(PhCH_2)SnCl$ (**6**).

of DMF. Each tin atom is pentacoordinate with a single DMF molecule coordinated via the O atom and no self-assembling can be observed in the packing diagram. All bond lengths are typical of such systems. It is interesting that Jurkschat et al. reported a similar system in which 1,2-bis(diphenylchlorotin)ethane reacted with HMPA. However, in this latter case only a single tin atom was coordinated by the HMPA ligand, while the other tin atom exhibited an interesting intramolecular secondary bond to the chlorine atom of the other tin group [15]. The greater distance between the two tin atoms in the case of **3** seems to preclude such bonding in the present case. A similar result was observed by Zobel et al. when two water molecules were coordinated, one at each tin atom of the related 1,3-bis(diphenylchlorotin)propane [16].

3.3. Biocidal evaluation

Given the significant anti-cancer activity reported for bis-organotin chloride compounds, i.e., $ClEt_2Sn–C_6H_4–p$-$SnEt_2Cl$ and $ClMe_2Sn–C_6H_4–p$-$SnMe_2Cl$ [3], we have performed a preliminary evaluation of the antibiotic activity of both **2** and **3** against *S. aureus*, *E. coli* and *P. phosphoreum*. Furthermore, we have compared this activity against that of the related mono-tin compounds $Ph_2(CH_3)SnCl$ (**5**) and $Ph_2(PhCH_2)SnCl$ (**6**) since both **2** and **3** contain the same basic organotin unit, $Ph_2Sn(Cl)CH_2–$. The minimum inhibitory concentration (MIC) of the chlorotin compounds against the three bacteria are presented in graphical form in Fig. 5. All four organotin chlorides exhibit the same selectivity of activity towards the three bacteria, i.e., *P. phosphoreum* > *S. aureus* > *E. coli*. In general the 1,4-bis(diphenylchlorotin)-butane (**2**) shows the greatest activity as might be expected by virtue of the two active tin centres when compared to the mono-tin compounds **5** and **6**. However, the obvious reduction in activity for the α,α^1-bis(diphenylchlorotin)xylene shows that the advantage of the extra tin atom is readily negated by replacing the flexible bridging butyl group with the more rigid phenyl group. More detailed studies are in progress to fully document and delineate the general biocidal activity of the series of diaryl(alkyl)tin chlorides and aryl(dialkyl)tin chlorides.

4. Supplementary material

Crystallographic data for the structural analyses have been deposited with the Cambridge Crystallographic Data Centre, CCDC 290345–290348, (**1**–**4**, respectively). Copies of this information may be obtained free of charge from The Director, CCDC, 12 Union Road, Cambridge, CB2 1EZ, UK, fax: +44 1223 336 033; email deposit@ccdc.cam.ac.uk or www: http://www,ccdc.cam.ac.uk.

Acknowledgements

This research was supported by the NIH-SCORE (GM-08012) and MARC (008048) programs and the Welch Foundation, Houston, Texas (Grant #AH-0546).

References

[1] M.A. Champ, P.F. Seligman, in: M.A. Champ, P.F. Seligman (Eds.), Organotin: Environmental Fate and Effects, Chapman & Hall, NY, 1996.
[2] (a) M.M. Whalen, B.G. Longanathan, K. Kannan, Environ. Res., Sect. A 81 (1999) 108;
(b) K. Kannan, K. Senthilkumar, J.P. Giesy, Environ. Sci. Technol. 33 (1999) 1776;
(c) A. Aluoch, M. Whalen, Toxicology 209 (2005) 263.
[3] (a) V.L. Narayanan, M. Nasr, K.D. Paull, NATO ASI Ser., Ser. H: Cell Biol. 37 (1990) 201;
(b) C.E. Carraher, Jr., D. Siegmann-Louda, Macromolecules Containing Metal and Metal-Like Elements, vol. 3, 2004, p. 57;
(c) D. Vos, R. Willem, M. Gielen, K.E. Van Wingerden, K. Nooter, Metal-Based Drugs 5 (1998) 179;
(d) M. Gielen, M. Biesemans, R. Willem, Appl. Organomet. Chem. 19 (2005) 440.
[4] M.A. Champ, Reported by A.M. Rouhi, Chem. Eng. News, American Chemical Society, Washington, DC. 76 (1998) 41.
[5] (a) H. Zimmer, H.G. Mosle, Chem. Ber. 87 (1954) 1255;
(b) Y. Azuma, M. Newcombe, Organometallics 3 (1984) 9.
[6] M. Gielen, K. Jurkschat, J. Organomet. Chem. 273 (1984) 303.
[7] B. Wrackmeyer, Ann. Rep. NMR Spectrosc. 16 (1985) 73.
[8] D. Dakternieks, Y. Farhangi, E.R.T. Tiekink, Zeit. fuer Kristallographie – New Cryst. Struct. 213 (1998) 397.
[9] National Committee for Clinical Laboratory Standards, Methods for Dilution Antimicrobial Susceptibility Tests for Bacteria that Grow Aerobically, fourth ed., Approved Standard, NCCLS Document M7-A4, NCCLS, Wayne, PA, 1997.
[10] D. Dakternieks, A.E.K. Lim, K. Jurkschat, E.R.T. Tiekink, Zeit. fuer Kristallographie – New Cryst. Struct. 214 (1999) 515.
[11] I. Haiduc, F.T. Edelmann, Supramolecular Organometallic Chemistry, Wiley–VCH, 1999 (Chapter 4).
[12] M.B. Hossein, J.L. Lefferts, K.C. Molloy, D. van der Helm, J.J. Zuckerman, Inorg. Chim. Acta 36 (1979) L409.
[13] K.C. Molloy, K. Quill, I.W. Novell, J. Organomet. Chem. 289 (1985) 271.
[14] U. Kolb, M. Drager, B. Jousseaume, Organometallics 10 (1991) 2737.
[15] K. Jurkschat, F. Hesselbarth, M. Dargatz, J. Lehmann, E. Kleinpeter, A. Tzschach, J. Organomet. Chem. 388 (1990) 259.
[16] B. Zobel, A. Duthie, D. Dakternieks, E.R.T. Tiekink, Organometallics 20 (2001) 2820.